Süleyman Demirel Üniversitesi Fen Edebiyat Fakültesi Fen Dergisi
Süleyman Demirel University Faculty of Arts and Sciences Journal of Science
2021, 16(2): 490-499
DOI: 10.29233/sdufeffd.933338
Atıf için / For Citation: Y. Gaylan, A. Bozkurt, B. Avar, "Investigating thermal and fast neutron shielding properties of B_4C-, B_2O_3-, Sm_2O_3-, and Gd_2O_3-doped polymer matrix composites using Monte Carlo simulations ", *Süleyman Demirel Üniversitesi Fen Edebiyat Fakültesi Fen Dergisi*, 16(2), 490-499, 2021.
Research Article

Investigating Thermal and Fast Neutron Shielding Properties of B_4C-, B_2O_3-, Sm_2O_3-, and Gd_2O_3-doped Polymer Matrix Composites using Monte Carlo Simulations

Yasin GAYLAN[*1], Ahmet BOZKURT[2], Barış AVAR[1,3]

[1]*Zonguldak Bülent Ecevit University, Graduate School of Science Engineering And Technology, Division of Nanotechnology Engineering, Zonguldak, 67100, Turkey*
[2]*Akdeniz University, Faculty of Engineering, Department of Biomedical Engineering, 07058, Antalya, Turkey*
[3]*Zonguldak Bülent Ecevit University, Faculty of Engineering, Department of Metallurgical and Materials Engineering, 67100, Zonguldak, Turkey*

**corresponding aouthor e-mail: yasingaylan@beun.edu.tr*

(Received: 05.05.2021, Accepted: 08.11.2021, Published: 25.11.2021)

Abstract: In this study, thermal ($2.53*10^{-8}$ MeV) and fast (2 MeV) neutron total macroscopic cross-sections of paraffin, polycarbonate, and polyester matrix polymers doped with B_4C, B_2O_3, Sm_2O_3, and Gd_2O_3 (at weight percentages of 5%, 10%, 15%, 20%, and 25%) were computed by using Monte Carlo simulations. Additionally, the macroscopic effective removal cross-section ($\sum_R$) of fast neutrons was theoretically computed based on the mass removal cross-section values ($\sum_R/\rho$) for various elements in polymers and additives. The obtained results show that the highest thermal neutron total macroscopic cross-section was obtained in polycarbonate doped with Gd_2O_3, and the highest fast neutron total macroscopic cross-section was observed in paraffin doped with Sm_2O_3. Besides, the paraffin provided the highest fast neutron total macroscopic cross-section for all additives. The results of this study provide a good understanding of shielding properties of paraffin, polycarbonate, and polyester matrix polymers doped with B_4C, B_2O_3, Sm_2O_3, and Gd_2O_3 against thermal and fast neutrons.

***Key words*:** Neutron shielding, Monte Carlo simulation, Polymer composite

Monte Carlo Simülasyonu Kullanılarak B_4C, B_2O_3, Sm_2O_3 ve Gd_2O_3 Katkılı Polimer Matrisli Kompozitlerin Termal ve Hızlı Nötron Zırhlama Özelliklerinin İncelenmesi

Öz: Bu çalışmada, B_4C, B_2O_3, Sm_2O_3 ve Gd_2O_3 katkılı (%5, %10, %15, %20 ve %25 ağırlık oranlarında) parafin, polikarbonat ve polyester matrisli polimerlerin termal ($2.53*10^{-8}$ MeV) ve hızlı (2 MeV) nötron toplam makroskopik tesir kesitleri Monte Carlo simülasyonu kullanılarak hesaplanmıştır. Ayrıca, hızlı nötronların makroskopik etkin ayırma tesir kesiti ($\sum_R$), polimerlerdeki ve katkı maddelerindeki elementlerin kütlesel ayırma tesir kesiti değerleri ($\sum_R/\rho$) kullanılarak teorik olarak da hesaplanmıştır. Elde edilen sonuçlar, en yüksek termal nötron toplam makroskopik tesir kesiti Gd_2O_3 katkılı polikarbonat ve en yüksek hızlı nötron toplam makroskopik tesir kesiti Sm_2O_3 katkılı parafin ile elde edildiğini göstermiştir. Bunun yanında parafinin, tüm katkı maddeleri için en yüksek hızlı nötron toplam makroskopik kesitine sahip olduğu görülmüştür. Bu çalışmanın sonuçları, B_4C, B_2O_3, Sm_2O_3 ve Gd_2O_3 katkılı parafin, polikarbonat ve polyester matrisli polimerlerin termal ve hızlı nötronlara karşı zırhlama özelliklerinin iyi bir şekilde anlaşılmasını sağlamıştır.

***Anahtar kelimeler*:** Nötron zırhlama, Monte Carlo simülasyonu, Polimer kompozit

Yasin GAYLAN, yasingaylan@beun.edu.tr, ORCID: https://orcid.org/0000-0003-1354-7593
Ahmet BOZKURT, abozkurt@akdeniz.edu.tr, ORCID: https://orcid.org/0000-0002-3163-0131
Barış AVAR, barisavar@beun.edu.tr, ORCID: https://orcid.org/0000-0002-6234-5448

1.Introduction

In recent years, neutron sources have been used in many applications such as neutron capture therapy [1], neutron imaging [2,3], elemental analysis [4], and nuclear power plants [5]. Since the radiation weighting factor of neutrons is higher than that of other types of indirectly ionizing radiations [6], shielding is considered a significant part of protection and safety practices for radiation workers and the public in applications involving neutron sources. For this purpose, many shielding materials have been developed, ranging from different types of concretes [7] to metal [8] and polymer [9] matrix composites, depending on the energy spectrum of the neutrons as well as the specific intent of the use, and thus a large body of similar work accordingly draws attention of the researchers worldwide.

Since neutrons are electrically neutral, they cannot be stopped by electromagnetic interactions like charged particles. Thus, the design process of neutron shields is basically considered in two stages: moderation and absorption [10]. Since the absorption cross-section of fast neutrons is considerably small, that is negligible in most cases, they are first slowed down with a suitable moderator and then are absorbed by nuclei with high absorption cross-sections for thermal neutrons.

During moderation, the kinetic energy (E_k) that a neutron will retain as a result of an elastic collision with an atomic nucleus is indicated by the formula,

$$E_k = \frac{4Mm}{4(M+m)}\cos\beta \qquad (1)$$

where M is the mass of the recoil nucleus, m is the mass of the incoming neutron, and β is the scattering angle of the nucleus with respect to the direction of the incoming neutron. The E_k values of some isotopes when $\beta = 0$ are given in Table 1 as a function of the nuclear mass of the isotopes expressed in atomic mass units (amu).

Table 1. Examples of neutron energy fraction as a function of recoil nuclear mass

Nucleus	Mass (M in amu)	E_k (%)
^{1}H	1.007825	100
^{2}H	2.014102	89
^{9}Be	9.012182	36.2
^{12}C	12.000000	28.6
^{16}O	15.994915	22.3
^{28}Si	27.976927	13.4
^{55}Mn	54.938047	7.1
^{197}Au	196.96654	2.0

According to Table 1, light elements are effective moderators for high-energy neutrons, and water consequently serves as a good neutron moderator due to its higher hydrogen content. However, the fact that water is liquid at room temperature becomes a disadvantage for neutron shielding purposes.

Polymers are good neutron moderators because of their properties such as high hydrogen content, solidity at room temperature, low Z, lightness, durability, shapeability, cheapness, and stability at a wide range of temperatures and are therefore considered as alternative shielding materials to water. While hydrogen is a good moderator, its neutron absorption cross-section is very low as indicated by the corresponding data in Table 4. Accordingly, many studies have been conducted to improve neutron absorption properties of polymers [11-13] where materials with a high thermal neutron macroscopic cross-section such as boron, cadmium, gadolinium, and samarium are usually added at varying proportions to further reduce the necessary shield thickness of the final material by increasing absorption of thermal

neutrons [14-18]. Woosley et al. found a 20% reduction in the thermal neutron flux after adding boron nitride to a thermoplastic polymer at the ratio of 20% [19]. Toyen et al. observed that by adding B_2O_3 to paraffin at varying ratios between 0 wt% to 35 wt%, the thermal neutron flux decreased from 95% to 30% [16]. In another study, Soltani et al. added 1 wt%, 2 wt% and 5 wt% boron to HDPE (high density polyethylene) and found that the macroscopic thermal neutron absorption cross-section increased from 0.29 cm^{-1} to 1.23 cm^{-1} [20]. Mesbahi et al. investigated the fast neutron cross-sections of polyurethane matrix of micro and nano sized polymers doped with B_4C, BeO, WO_3, ZnO, and Gd_2O_3 and observed that nanoscale doping increased the fast neutron cross-section [21]. Besides, there are studies aiming to improve the gamma ray linear attenuation coefficient by doping polymers in the literature [9,22].

In this study, thermal ($2.53*10^{-8}$ MeV) and fast (2 MeV) neutron total macroscopic and removal cross-sections of some composites formed by doping several polymers as seen in Table 2 (paraffin, plycarbon, and polyester) with B_4C, B_2O_3, Sm_2O_3 and Gd_2O_3 at the ratios of 5 wt%, 10 wt%, 15 wt%, 20 wt%, and 25 wt% were calculated using the MCNP5 code package developed to employ the Monte Carlo technique for simulating transport of radiation particles in material media.

Table 2. Elemental weight fraction of the polymers investigated in this study

Element	**Paraffin ($C_{25}H_{52}$)**[23]	**Polycarbonate ($C_{16}H_{14}O_3$)** [23]	**Polyester ($C_{16}H_{14}O_7$)** [24]
H	0.148605	0.055491	0.044025
C	0.851395	0.755751	0.603773
O	-	0.188758	0.352201

2. Materials and Methods

2.1 Monte Carlo Simulations

Statistical models like the Monte Carlo technique offer good numerical alternatives for solving physical problems when experimental conditions are either limited or difficult to perform. The MCNP code (the Monte Carlo N-particle radiation transport code), version 5, is a simulation program that can handle three-dimensional geometries and has wide applications in areas such as shielding, reactor design, dose calculations, and medical imaging [25]. In the literature, MCNP has been to calculate radiation protection performance of various materials such as concretes [26], glasses [27], and metal composites [28]. In this study, we used the MCNP5 version of the code for computing thermal and fast neutron total macroscopic cross-sections of some candidate shielding materials.

As shown in Figure 1, the simulation geometry consists of a mono-energetic point neutron source placed in a cylindrical cavity, target material and detector (F4 Tally) to measure the neutron flux through the material in vacuum.

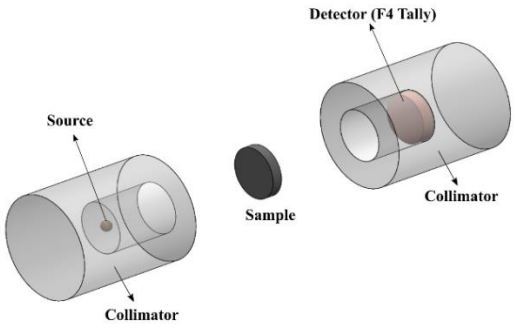

Figure 1. Geometry of the simulation setup

The target materials considered in this study were created by homogeneously mixing polymer materials as the base matrix and various compounds with high thermal neutron cross-section were added at different weight percentages. Paraffin ($C_{25}H_{52}$, density = 0.93 g/cm^3), polycarbonate ($C_{16}H_{14}O_3$, density = 1.2 g/cm^3), and polyester ($C_{16}H_{14}O_7$, density = 1.12 g/cm^3) were selected as matrix materials. B_4C (density = 2.52 g/cm^3), B_2O_3 (density = 1.81 g/cm^3), Sm_2O_3 (density = 8.35 g/cm^3), and Gd_2O_3 (density = 7.41 g/cm^3) were used as the additives. The doping ratios for each additive were set at 5 wt%, 10 wt%, 15 wt%, 20 wt%, and 25 wt%. The thermal neutrons were defined at $2.53*10^{-8}$ MeV while the fast energy neutrons were set as having 2 MeV. In order to shorten the simulation run time, the photon importance was set to 0 and thus no photon was created as a result of neutron interactions with the absorbers. The distance between the neutron source and the target material, as well as the distance between the target material and the detector were both set as 50 cm. The detector cell and target material were designed as a cylinder. The detector flux was calculated using the F4 tally of MCNP5, which measures average flux per cm^2 per source particle. Before each simulation, the flux I_0 was calculated when no target material was present, and then the flux I_x was calculated by inserting the target material between the source and the detector. In the simulations, 10^7 neutron histories were created and the statistical error was below 1%.

2.2 Calculation of Total Macroscopic Cross-Section ($\sum_t$)

As neutrons pass through a scattering or absorbing medium, they can interact in various ways depending on their energy and the nuclei of the atoms in the material. The basic interactions between the neutron and the nucleus include elastic scattering, inelastic scattering, neutron capture, and nuclear fission. The microscopic cross-section (σ_t), which refers to the total probability of a neutron of a certain energy to interact with the atoms in the medium it passes through by one of the above mechanisms, is defined as the sum of the microscopic cross-sections for scattering (σ_s) and absorption interactions (σ_a).

$$\sigma_t = \sigma_a + \sigma_s \tag{2}$$

The absorption of neutrons as they pass through a matter depends not only on the microscopic cross-section but also on the number density of the absorbing nuclei in the material. The physical quantity containing these two parameters is denoted by $\sum_t$ and is called the total macroscopic cross-section [5]

$$\sum_t = N\sigma_t \tag{3}$$

where N is the number of nuclei per unit volume and the unit of $\sum_t$ is cm^{-1}.

In cases of different nuclei mixed together in a material, the total macroscopic cross-section is calculated by the mixture formula as follows:

$$\sum_t = N_a\sigma_a + N_b\sigma_b + N_c\sigma_c + \cdots \quad (4)$$

where N_a, N_b and N_c are the number of nuclei in elements A, B and C per unit volume.

To determine $\sum_t$ of a material, the intensity of the neutron beam that gets attenuated due to absorption and scattering when passing through a medium of material is needed, along with the intensity of neutrons when there is no absorber. The attenuation by the medium is then calculated by the well-known Beer-Lambert law [29]:

$$I_X = I_0 e^{-\sum_t x} \quad (5)$$

where I_0 and I_x are, respectively, the intensity of the incoming neutrons (emitted from the source) and the intensity of the neutrons passing through the absorber, *x* (cm) is the absorber thickness, and $\sum_t$ is the total macroscopic cross-section of the absorbing medium. If in this equation, I_0 and I_x can be determined either through measurements or simulations for a known thickness of an absorber, $\sum_t$ of the material can then be readily determined.

2.3 Calculation of Fast Neutron Effective Removal Cross-Section ($\sum_R$)

The fast neutron effective removal cross-section (called removal cross-section) $\sum_R$ (cm^{-1}), is the probability that a fast or fission energy neutron undergoes a first collision, which removes it from the group of penetrating, uncollided neutrons. The removal cross-section is considered to be approximately constant for neutron energies between 2 and 12 MeV, and may be calculated for various elements in the compounds or mixtures by the general formula [30,31]

$$\sum_R = \sum_i \rho_i (\sum_R/\rho)_i \quad (6)$$

where ρ_i and $(\sum_R/\rho)_i$ are, respectively, the partial density (g cm^{-3}), and the mass removal cross-section of the ith constituent ($cm^2.g^{-1}$), compound or simple element.

It is worth mentioning that the partial density ρ_i is given by the product of weight fraction W_i of the *i*th element and the density of the sample ρ_s as follow:

$$\rho_i = W_i \ \rho_s \quad (7)$$

The $(\sum_R/\rho)$ values of the elements used in this study is shown in Table 3.

Table 3. The mass removal cross-sections of elements

Element	$\sum_R/\rho$ ($cm^2\ g^{-1}$)
H	0.598
B	0.0575
C	0.0502
O	0.0405
Gd	0.0119
Sm	0.0121

3. Results and Discussion

Figures 2(a-c) show the calculated thermal neutron total macroscopic cross-sections for paraffin, polycarbonate, polyester matrix materials depending on the doping ratio of B_4C, B_2O_3, Sm_2O_3, and Gd_2O_3. While the thermal neutron total macroscopic cross-section of pure paraffin was 2.86 cm^{-1}, it was found to increase up to 15.88 cm^{-1} with the addition of B_4C, up

to 6.84 cm^{-1} with the addition of B_2O_3, up to 21.41 cm^{-1} with the addition of Sm_2O_3, and up to 102.52 cm^{-1} with the addition of Gd_2O_3. While the thermal neutron total macroscopic cross-section of pure polycarbonate was 1.62 cm^{-1}, it was found to increase up to 15.72 cm^{-1} with the addition of B_4C, up to 6.31 cm^{-1} with the addition of B_2O_3, up to 19.31 cm^{-1} with the addition of Sm_2O_3, and up to 107.23 cm^{-1} with the addition of Gd_2O_3. Finally, the thermal neutron total macroscopic cross-section of pure polyester was 1.27 cm^{-1} and was found to increase up to 14.87 cm^{-1} with the addition of B_4C, up to 5.82 cm^{-1} with the addition of B_2O_3, up to 18.45 cm^{-1} with the addition of Sm_2O_3, and up to 104.48 cm^{-1} with the addition of Gd_2O_3. Adeli et al. [32] observed that doping polymers with 5 wt% B_4C increased the thermal neutron cross-section from 0.076 cm^{-1} to 0.345 cm^{-1} depending on the particle size of B_4C.

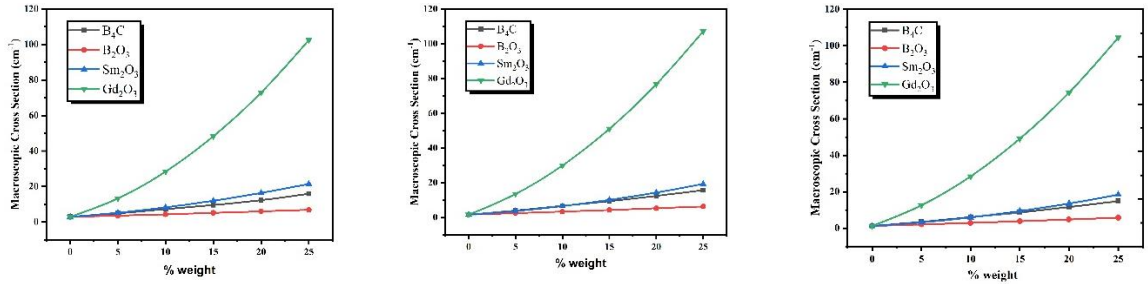

(a) (b) (c)

Figure 2. Thermal neutron total macroscopic cross-sections of (a) paraffin, (b) polycarbonate and (c) polyester matrix materials as a function of doping percentages.

The fast neutron total macroscopic cross-sections depending on the mixing ratio by weight are shown in Figure 3 (a-c). The results reveal that paraffin matrix materials had the highest fast neutron total macroscopic cross-section for all doping ratios and for all additives. In addition, Aygün and Budak examined the fast neutron cross-section of paraffin wax according to the oil percentage and observed that the fast neutron cross-section of paraffin wax increased as the amount of oil increased [33]. Sm_2O_3 turned out to have the highest fast neutron total macroscopic cross-section for all doping raitos in all polymers. Doping with B_2O_3 yielded the highest fast neutron total macroscopic cross-section for paraffin and polycarbonate at 10% by weight and for polyester at 15% by weight. This behavior was due to the Gd, Sm and B elements having a considerable higher thermal neutron cross-section values. In a similar study, Tuna et al. [34] also observed that increasing the amount of B_4C increased the fast neutron absorption rate of polyester.

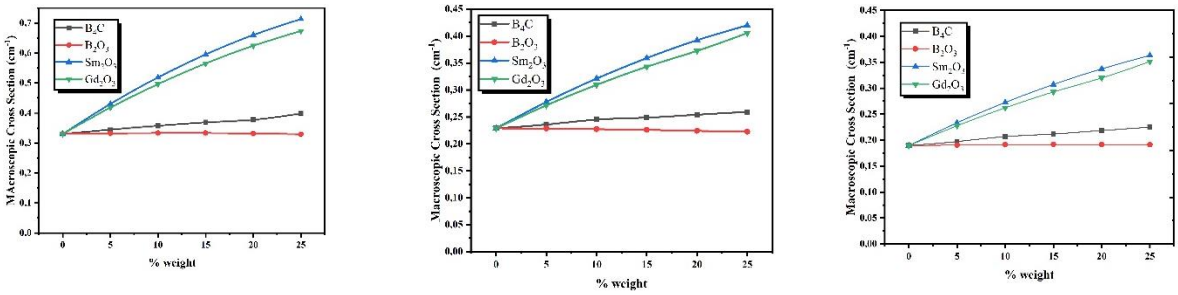

(a) (b) (c)

Figure 3. Fast neutron total macroscopic cross-sections of (a) paraffin, (b) polycarbonate and (c) polyester matrix materials as a function of doping percentages.

The removal cross-sections theoretically calculated according to Eq. 6 are shown in Figure 4(a-c). In paraffin samples, doping with 25% Sm_2O_3 resulted the highest increase as 134%, while doping with 25% B_2O_3 resulted the lowest increase as 4%. The $\sum_R$ values of paraffin and polycarbonate are higher than the $\sum_R$ value of ordinary concrete reported by Bashter [35].

From the previous literature review, the highest removal cross section was found in paraffin with more than 10wt% contents of Sm_2O_3 and Gd_2O_3, and polycarbonate with 25wt% content of Sm_2O_3 [11,12].

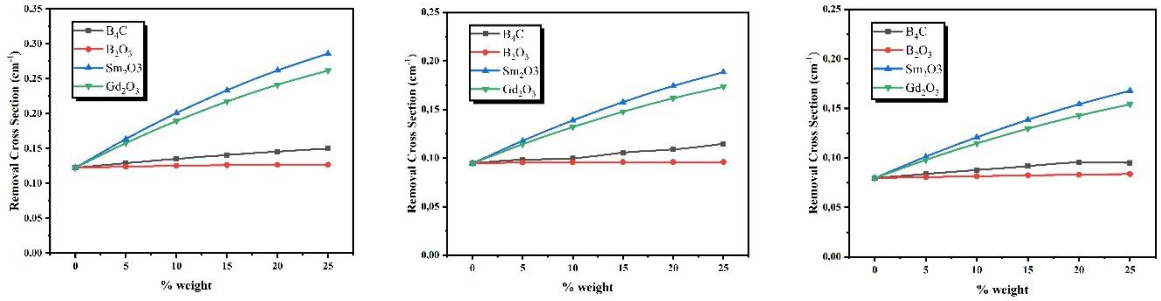

(a) (b) (c)

Figure 4. Neutron removal cross-sections of (a) paraffin, (b) polycarbonate and (c) polyester matrix materials as a function of doping percentages.

The thermal and fast neutron cross-section values of the elements used in our study are shown in Table 4. The reason why Gd_2O_3 doping has the highest thermal neutron total macroscopic cross-section value in all polymers can be explained by higher thermal neutron cross-section of Gd, as can be seen in Table 4. Likewise, Sm_2O_3 doping has the second highest thermal neutron total macroscopic cross-section value in all polymers after Gd_2O_3. It has a high thermal neutron total macroscopic cross-section due to boron content of B_4C and B_2O_3. B_4C contains boron 80% by weight and B_2O_3 31% by weight. Therefore, it is seen that the lowest thermal neutron total macroscopic cross-section in all polymers is in B_2O_3 doped polymers.

As can be seen in Table 1 and Table 4, the hydrogen rich polymers are effective in shielding fast neutrons. For this reason, it stands out in fast neutron shielding with its 14% hydrogen value in paraffin content. Although, the gadolinium has high total cross-section for fast neutron, samarium doped materials have the high value in cross-section calculations. This is because the density of Sm_2O_3 is higher than Gd_2O_3.

Table 4. Neutron cross-sections (barn) of the elements or isotopes included in this study

Isotope / Element	**Thermal neutrons (0.0253 eV)**			**Fast neutrons (2 MeV)**
	Total cross-section [36]	Absorption cross-section [37]	Total bound scattering cross-section [37]	Total cross-section [36]
H	30.6011	0.3326	82.02	2.90841
B-10	3847	3835	3.1	2.15983
B-11	5.07207	0.0055	5.77	1.95305
C-12 (98.91)	4.956	0.00353	5.559	1.70921
C-13 (1.07)	5.90679	0.00137	4.84	1.64815
O	3.91631	0.00019	4.232	1.5796
Natural Gd	48739.15	49700	180	6.682
Natural Sm	5704.971	5922	39	6.565774

4. Conclusions and Comment

This study has investigated the changes in the thermal neutron total macroscopic, fast neutron total macroscopic and removal cross-sections of paraffin, polycarbonate, and polyester in

response to doping with B_4C, B_2O_3, Sm_2O_3, and Gd_2O_3 at varying proportions. The results can be summarized as the following:

1. Paraffin yielded the highest fast neutron total macroscopic and removal cross-section values since it has a higher hydrogen content by weight in comparison to polycarbonate and polyester.
2. Paraffin has the highest thermal neutron total macroscopic cross-section when doped with B_4C, B_2O_3, and Sm_2O_3, while the polycarbonate has the highest thermal neutron total macroscopic cross-section when doped with Gd_2O_3.
3. This study has provided us with information on changes in the thermal and fast neutron total macroscopic cross-sections depending on the content of the material doped with polymer matrix composites and on the doping ratio. It can be concluded that materials to be used for neutron shielding should be produced and their physical properties should be examined considering both their thermal and fast neutron total macroscopic cross-sections.

Author Statement

Yasin Gaylan: Investigation, Original Draft Writing, Review and Editing,
Ahmet Bozkurt: Resource/Material/Instrument, Review and Editing, Supply, Supervision
Barış Avar: Project Management, Investigation, Review and Editing, Supervision

Acknowledgment

We would like to thank Zonguldak Bülent Ecevit University (Project no. 2020-73338635-01) for the financial support.

Conflict of Interest

As the authors of this study, we declare that we do not have any conflict of interest statement.

Ethics Committee Approval and Informed Consent

As the authors of this study, we declare that we do not have any ethics committee approval and/or informed consent statement.

References

[1] S. Chandra, T. Ahmad, R. F. Barth, and G. W. Kabalka, "Quantitative evaluation of boron neutron capture therapy (BNCT) drugs for boron delivery and retention at subcellular-scale resolution in human glioblastoma cells with imaging secondary ion mass spectrometry (SIMS)," *J. Microsc.*, 254 (3), 146–156, 2014, doi: 10.1111/jmi.12126.

[2] D. Kramer *et al.*, "In situ diagnostic of two-phase flow phenomena in polymer electrolyte fuel cells by neutron imaging: Part A. Experimental, data treatment, and quantification," *Electrochim. Acta*, 50 (13), 2603–2614, 2005, doi: 10.1016/j.electacta.2004.11.005.

[3] J. Zhang *et al.*, "In situ diagnostic of two-phase flow phenomena in polymer electrolyte fuel cells by neutron imaging: Part B. Material variations," *Electrochim. Acta*, 51 (13), 2715–2727, Mar. 2006, doi: 10.1016/j.electacta.2005.08.010.

[4] A. Ittipongse and R. Fungklin, "Neutron activation for analyzing elements in material," in *Key Engineering Materials*, 675–676, 700–703, 2016, doi: 10.4028/www.scientific.net/KEM.675-676.700.

[5] J. E. Martin, *Physics for Radiation Protection, Third Edition*. Wiley-VCH, 2013.

[6] ICRP, "Annals of the International Commission on Radiological Protection, ICRP Publication 103," *Ann. ICRP*, 37, 3–4, p. 332, 2007.

[7] O. Gencel, A. Bozkurt, E. Kam, and T. Korkut, "Determination and calculation of gamma and neutron shielding characteristics of concretes containing different hematite proportions," *Ann. Nucl. Energy*, 38

(12), 2719–2723, 2011, doi: 10.1016/j.anucene.2011.08.010.
[8] A. Akkas, A. B. Tugrul, B. Buyuk, A. O. Addemir, M. Marsoglu, and B. Agacan, "Shielding effect of boron carbide aluminium metal matrix composite against gamma and neutron radiation," *Acta Phys. Pol. A*, 128 (2), 176–179, 2015, doi: 10.12693/APhysPolA.128.B-176.
[9] S. D. Kaloshkin, V. V. Tcherdyntsev, M. V. Gorshenkov, V. N. Gulbin, and S. A. Kuznetsov, "Radiation-protective polymer-matrix nanostructured composites," *J. Alloys Compd.*, 536 (SUPPL.1), S522–S526, 2012, doi: 10.1016/j.jallcom.2012.01.061.
[10] A. B. Chilton, J. K. Shultis, and R. E. Faw, *Principles of Radiation Shielding*. Prentice-Hall, 1984.
[11] C. V. More, Z. Alsayed, M. S. Badawi, A. A. Thabet, and P. P. Pawar, "Polymeric composite materials for radiation shielding: a review," *Environ. Chem. Lett.*, 19, 2057-2090, 2021.
[12] M. R. Kaçal, F. Akman, and M. I. Sayyed, "Evaluation of gamma-ray and neutron attenuation properties of some polymers," *Nucl. Eng. Technol.*, 51 (3), 818–824, 2019, doi: 10.1016/j.net.2018.11.011.
[13] B. Körpınar, B. Canbaz Öztürk, N. F. Çam, and H. Akat, "Radiation shielding properties of Poly(hydroxylethyl methacrylate)/Tungsten(VI) oxide composites," *Mater. Chem. Phys.*, 239 (January), 2020, doi: 10.1016/j.matchemphys.2019.121986.
[14] G. İrim *et al.*, "Physical, mechanical and neutron shielding properties of h-BN/Gd2O3/HDPE ternary nanocomposites," *Radiat. Phys. Chem.*, 144 (March), 434–443, 2018, doi: 10.1016/j.radphyschem.2017.10.007.
[15] P. Wang, X. Tang, H. Chai, D. Chen, and Y. Qiu, "Design, fabrication, and properties of a continuous carbon-fiber reinforced Sm2O3/polyimide gamma ray/neutron shielding material," *Fusion Eng. Des.*, 101, 218–225, 2015, doi: 10.1016/j.fusengdes.2015.09.007.
[16] D. Toyen and K. Saenboonruang, "Development of paraffin and paraffin/bitumen composites with additions of B2O3 for thermal neutron shielding applications," *J. Nucl. Sci. Technol.*, 54 (8), 871–877, 2017, doi: 10.1080/00223131.2017.1323688.
[17] N. R. Abd Elwahab, N. Helal, T. Mohamed, F. Shahin, and F. M. Ali, "New shielding composite paste for mixed fields of fast neutrons and gamma rays," *Mater. Chem. Phys.*, 233 (May), 249–253, 2019, doi: 10.1016/j.matchemphys.2019.05.059.
[18] Z. Uddin, T. Yasin, M. Shafiq, A. Raza, and A. Zahur, "On the physical, chemical, and neutron shielding properties of polyethylene/boron carbide composites," *Radiat. Phys. Chem.*, 166 (January), 108450, 2020, doi: 10.1016/j.radphyschem.2019.108450.
[19] S. Woosley, N. Abuali Galehdari, A. Kelkar, and S. Aravamudhan, "Fused deposition modeling 3D printing of boron nitride composites for neutron radiation shielding," *J. Mater. Res.*, 33 (22), 3657–3664, 2018, doi: 10.1557/jmr.2018.316.
[20] Z. Soltani, A. Beigzadeh, F. Ziaie, and E. Asadi, "Effect of particle size and percentages of boron carbide on the thermal neutron radiation shielding properties of HDPE/B4C composite: Experimental and simulation studies," *Radiat. Phys. Chem.*, 127, 182–187, 2016, doi: 10.1016/j.radphyschem.2016.06.027.
[21] A. Mesbahi, K. Verdipoor, F. Zolfagharpour, and A. Alemi, "Investigation of fast neutron shielding properties of new polyurethane-based composites loaded with B4C, BeO, WO3, ZnO, and Gd2O3 micro- and nanoparticles," *Polish J. Med. Phys. Eng.*, 25, (4), 211–219, Dec. 2019, doi: 10.2478/pjmpe-2019-0028.
[22] R. Biswas, H. Sahadath, A. S. Mollah, and M. F. Huq, "Calculation of gamma-ray attenuation parameters for locally developed shielding material: Polyboron," *J. Radiat. Res. Appl. Sci.*, 9 (1), 26–34, 2016, doi: 10.1016/j.jrras.2015.08.005.
[23] R. G. Williams, C. J. Gesh, and R. T. Pagh, "Compendium of Material Composition Data for Radiation Transport Modeling," Richland, WA, Oct. 2006. doi: 10.2172/902408.
[24] F. Özkalaycı, M. R. Kaçal, O. Agar, H. Polat, A. Sharma, and F. Akman, "Lead(II) chloride effects on nuclear shielding capabilities of polymer composites," *J. Phys. Chem. Solids*, 145 (January), 109543, 2020, doi: 10.1016/j.jpcs.2020.109543.
[25] M. C. Team, "MCNP-A General Monte Carlo N-Particle Transport Code, Version 5 Volume I: Overview and Theory X-5 Monte Carlo Team," 2003.
[26] M. I. Sayyed, K. A. Mahmoud, S. Islam, O. L. Tashlykov, E. Lacomme, and K. M. Kaky, "Application of the MCNP 5 code to simulate the shielding features of concrete samples with different aggregates," *Radiat. Phys. Chem.*, 174 (September), 108925, 2020, doi: 10.1016/j.radphyschem.2020.108925.
[27] R. El-Mallawany, M. I. Sayyed, M. G. Dong, and Y. S. Rammah, "Simulation of radiation shielding properties of glasses contain PbO," *Radiat. Phys. Chem.*, 151, 239–252, Oct. 2018, doi: 10.1016/j.radphyschem.2018.06.035.
[28] J. J. Park, S. M. Hong, M. K. Lee, C. K. Rhee, and W. H. Rhee, "Enhancement in the microstructure and neutron shielding efficiency of sandwich type of 6061Al-B 4 C composite material via hot isostatic pressing," *Nucl. Eng. Des.*, 282, 1–7, 2015, doi: 10.1016/j.nucengdes.2014.10.020.
[29] A. T. Boothroyd, *Principles of Neutron Scattering from Condensed Matter*. Oxford University Press, 2020.

[30] M. F. Kaplan, *Concrete radiation shielding : nuclear physics, concrete properties, design and construction*. Longman Scientific & Technical, 1989.
[31] A. E. Profio, *Radiation Shielding and Dosimetry*. Wiley, 1979.
[32] R. Adeli, S. Pezhman, and S. Javad, "Neutron irradiation tests on B4C/epoxy composite for neutron shielding application and the parameters assay," *Radiat. Phys. Chem.*, 127, 140–146, 2016, doi: 10.1016/j.radphyschem.2016.06.026.
[33] B. Aygün and G. Budak, "A new neutron absorber material : Oil loaded paraffin wax," *Nucl. Sci. Technol.*, 33–39, 2012.
[34] T. Tuna, A. A. Eker, and E. Kam, "Neutron shielding characteristics of polymer composites with boron carbide," *J. Korean Phys. Soc.*, 78 (7), 566–573, 2021, doi: 10.1007/s40042-021-00089-z.
[35] I. I. Bashter, "Calculation of radiation attenuation coefficients for shielding concretes," *Ann. Nucl. Energy*, 24, (17), 1389–1401, Nov. 1997, doi: 10.1016/S0306-4549(97)00003-0.
[36] "Nuclear Data Center at KAERI." http://atom.kaeri.re.kr/ (accessed Apr. 18, 2021).
[37] V. F. Sears, "Neutron scattering lengths and cross sections," *Neutron News*, 3 (3), 26–37, 1992, doi: 10.1080/10448639208218770.